Nanotubes stretched in liquid-metal-ion-sources and their influence on isotopic anomalies

P. Joyes, J. Van de Walle, and R.-J. Tarento
Laboratoire de Physique des Solides, batiment 510, Université d'Orsay, 91405 Orsay Cedex, France
(Received 5 December 2005; revised manuscript received 1 March 2006; published 31 March 2006)

The present paper argues that an intense electric field (few V/Å) provides an alternative method to stretch matter and to form nanotubes locally. The very high electric field is supplied by a liquid-metal-ion-source (LMIS). Intriguing aspects are displayed by the LMIS mass spectra of some pure elements. The periodicity of pure Ge or Sn LMIS, i.e., series of equidistant peaks such $Ge_{6n+1}{}^{3+}$ with $n=3-8$ or $Ge_{6n+4}{}^{3+}$ with $n=7-14$ or the formation of unexplained $Au_8{}^{3+}$ and $Au_{16}{}^{3+}$ ions for the pure Au LMIS, is attributed to the existence of Ge, Sn, or Au nanotubes in operating LMIS. LMIS results on a eutectic $Au_{0.73}Ge_{0.27}$ alloy show the formation of a gold nanotube associated with the strong $Au_8{}^{3+}$ emission. The $Ge_2{}^+$ emitted near the gold nanotube interacts with a larger electric field than in the pure Ge LMIS provoking a bond break in heteroisotope dimers and therefore isotope anomalies in dimer emission.

DOI: 10.1103/PhysRevB.73.115436 PACS number(s): 79.20.Rf

Nanotubes (NTs) and nanowires (NWs) have attracted much interest in recent years due to their importance both in electronic device technology and in fundamental physics. After the discovery of carbon NTs,[1] many other elements or compounds such as gold[2,3] were found to develop similar NW structures, where NWs are generally attached at their two extremities. Various modes of NW formation have been reported. One method[2,4] to get such NWs is to stretch the matter by withdrawing from a substrate a scanning tunneling tip on which suspended NWs are observed *in situ* by high-resolution transmission electron microscopy (HRTEM). HRTEM provides another method[3] to generate NWs by focusing the electron beam on a supported film until a nanometric neck is formed inside or between grains. To form or to establish the existence of NWs, alternative methods that do not use HRTEM are available. One is based on a mechanically controllable break (MCB) junction.[5] The NW is obtained from a notched sample that is broken by bending its support. The Leiden group[5,6] records its conductivity, which displays jumps of the order of $2e^2/h$ and reports electronic shell and supershell structures in alkali-metal NWs for which Jahn-Teller distortions[7] have been recently predicted. They succeed to form NWs for the 5*d* metal (Au,Pt,Ir) but not for the 4*d* or 3*d* metal (Pd,Ag,Rh).[8] They suggest that the origin of these results is due to relativistic effects in the *s*-*d* competition. Tosatti *et al.*[9] have pointed out the importance on the NW properties of the contacts at the NW extremities. Our paper deals with a new way to form NTs, in particular for elements of which the NW existence was previously reported. The NW structures most similar to ours are those obtained in MCB.

It is well known that intense electric fields applied to a viscous medium such as a liquid metal induce deformations inside the material. This paper shows that an intense electric field provides an alternative method to stretch the matter and to form a NT. Our intense electric field is provided by a liquid-metal-ion-source (LMIS). In the first part, we report results on NTs stretched from either pure gold or pure germanium LMIS. In the second part, the analysis of Au-Ge alloy LMIS experiments with eutectic composition concludes to the formation of gold NT and an enhancement of Ge^+ and $Ge_2{}^+$ emission from a region near the bottom of the NT. Isotopic anomalies in germanium dimer emission from a Ge-Au alloy previously reported[10] are shown to be related to the presence of gold NT.

Let us briefly describe the LMIS main features. A solid tip made of a refractory metal (for example, W) is wetted by a molten metal that is submitted to a high electric field at the end of the tip (few V/Å). Thus the electrostatic pressure is higher than the liquid superficial tension. An instability occurs in the apex region of the liquid leading to a Taylor cone formation, from where a field emission of particle or cluster occurs. LMIS is used mainly in technical applications to implant doping elements in electronic device. Due to the surface charge, the Taylor cone is deformed and is stretched as seen in Fig. 1. High voltage transmission electron microscope (HVTEM) observations by Benassayag, Sudraud, and Jouffrey[11] on operating LMIS show that extremely thin jets are produced. Diameters as small as 3 nm were observed which are only five times the diameter of typical one-shell NTs with a six-atom hexagonal section. Classical calculations developed by Swanson and Kingham[12] or Forbes[13] also lead to this order of magnitude. The preliminary conclusion of these two studies is that jet structures do exist. However, it is very hard to draw the exact jet size and structure at the atomic scale with HVTEM due to the intensity fluctuation in

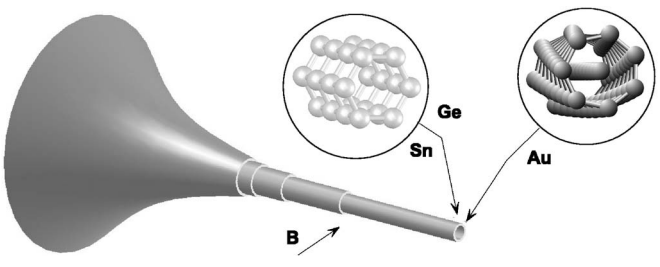

FIG. 1. Schematic representation of a LMIS jet shrinking by steps down to the atomic size of the thinnest nanowire. In the inset, the atomic geometry of the tip is displayed either for Au or for Ge and Sn. The Ge^+, $Ge_2{}^+$ are emitted in the eutectic Au-Ge LMIS from the region B as discussed in the text.

the emission. Moreover, the theoretical models based on classical physics have some limitations. In particular, they do not take into account the nature of the chemical bond. To go beyond and get more insight into the atomic geometric structure, we have to analyze the mass spectra of the emitted particles and clusters to confirm our conjecture that NTs exist in performing LMIS as drawn in Fig. 1. The largest part of monatomic and polyatomic emitted species in LMIS is monocharged. Two main parallel processes control these ion formations; they are either directly extracted from the surface, as occurs chiefly for the smallest ones, or produced by the explosion of metastable droplets at some distance of the tip mostly for the largest ones.[14] The very thin cylindrical NT jets are also a possible source of emission. At the top of this structure, the curvature is larger than in any other emitting region of the tip, therefore the charge density and the electric field are much stronger. We expect that the emitted ions from this cylindrical structure are characterized by a large $p+$ charge ($p>1$). Moreover, the matter being stretched along the field direction, large interatomic spacings appear and bonding is weaker along the cylindrical axis. Consequently, the electric field will easily extract slices of matter as in a cleavage. Suppose now that the highest part of the tip (see Fig. 1) has a section of ν atoms. Then we can expect the emission of $X_{m\nu}^{p+}$ ions with $p>1$, m varying with the slice width.

One remark is in order: the LMIS apex is far from equilibrium. The exact liquid or solid nature of the NT in LMIS is still not known but in our interpretation the NT is assumed to be close to solid order. This order is associated to the intense electric field which sets a cylindrical symmetry, and confines and orders matter perpendicularly to its axis in a cylinder structure of a few Å radius.

It seems natural to think that the NT geometry at the tip end depends on the nature of the bond. We shall discuss two results, one on covalent elements (Ge,Sn,Bi), which are known to favor directional bonds, and another using gold, which is expected to have a more compact structure.

The LMIS mass spectra obtained for germanium [Fig. 2(a)] and tin[15] [Fig. 3(a)] show a remarkable modulo-6 periodicity with peaks for X_{6n+1}^{+}, $n=3-8$. This result reveals a jet in operating LMIS from NT with a $\nu=6$ hexagonal section (see the inset in Fig. 1). In the case of germanium, a second series of $Ge_{6n+4}{}^{3+}$, $n=7-14$ is also observed. We notice that additional atoms (one in the first series, four in the Ge second series) are present in the emitted aggregates. These are due to the presence of a cap. In the first series, the cap is built up with one atom located along the NT axis and in the second series the cap is triangular with one atom on top. Due to some constraints, the four-atom cap occurs for clusters with larger slices. Note that for $n=7$ and 8, the two Ge types of caps are detected.

Let us pause to mention that in our interpretation we have dismissed some others that are less convincing. For instance, one is based on the idea that the top of the cone has just the radius of the NT. With this assumption, the formation of one six-atom germanium ring is plausible but the stacking of a large number of rings going to $n=14$ for $Ge_{6n+4}{}^{3+}$ is not easy to understand due to the high cluster charge, which is not in favor of a time sequential growth process by accretion of individual rings in an intense electric field zone. Let us mention another point: in our interpretation, mostly $Ge_{6n+1}{}^{3+}$ and $Ge_{6n+4}{}^{3+}$ species are emitted from the NT. We could derive a flow velocity (V_{flow}) of the mass transport near the apex to build continuously the NT, which yields the $Ge_{6n+1}{}^{3+}$ and $Ge_{6n+4}{}^{3+}$. For pure Ge, LIMS V_{flow} is 85 m/s, which seems to be a reasonable speed, thus this result does not invalidate our hypothesis.

The LMIS mass spectrum of bismuth[16] [Fig. 3(b)] also exhibits a periodicity for highly charged species with peaks for $Bi_{8n+3}{}^{3+}$, $n=2-5$, which are explained by jets from NW with an eight-atom section. The change of section from six to eight atoms reveals the decrease of the sp^2 character of the Bi bond in favor of the p character.

Let us examine the gold case. The nature of the chemical bond is expected to be metallic and the geometric structure to be more compact. This is confirmed by conductance measurements of thin NTs made simultaneously with high-resolution transmission electron microscopy (HRTEM) observations which report "magic radii." The NW has a multishell cylindrical structure. Let us focus on the smallest one, i.e., the two-shell gold NW. It has a central row of atoms and a second shell of seven atoms and it displays helicity (see the inset in Fig. 1). The gold LMIS mass spectrum [Fig. 2(b)] presents chiefly monocharged species. The peak intensities of the clusters $Au_n{}^{+}$ decrease with n. However, notice that the decrease of intensity from an even n-value to an odd one is smaller than from an odd n-value to an even one. This fact is explained if the gold atoms give one electron to form the chemical bond; therefore, the clusters $Au_{2n+1}{}^{+}$ with closed electronic level structure are more stable than the clusters $Au_{2n}{}^{+}$ with one unpaired electron. Let us concentrate our attention on the two multicharged peaks $Au_8{}^{3+}$ and $Au_{16}{}^{3+}$ both absent in the spectra of gold clusters yielded by sputtering techniques. Note that for the species $Au_{8n}{}^{3+}$ with $n\geqslant 3$, it is difficult to discuss their formation from our experiments because either our detection is limited in mass or is at the resolution limit for $Au_{24}{}^{3+}$. These two peaks $Au_8{}^{3+}$ and $Au_{16}{}^{3+}$ are intriguing. First, they do not correspond to some reported magic closed-shell electronic structure for metallic cluster, and secondly, they display an odd number of charges. Their detection suggests that they are associated with one or two slices of a section of eight atoms emitted from the two-shell gold NT.

As seen before, pure gold or pure germanium LMIS lead to gold or germanium NT formation. An intriguing question is the following: at the atomic scale, what is the geometric structure of the tip in a Au-Ge alloy LMIS? Our alloy has the eutectic composition $Au_{0.73}Ge_{0.27}$. In Fig. 2(c), the emission spectra of the Au-Ge alloy LMIS gives some insights. First the pure gold clusters $Au_n{}^{p+}$ are emitted nearly as in the pure gold LMIS. In particular, $Au_8{}^{3+}$, which has been associated with gold NTs, is present, its shape is slightly better resolved than in the pure Au case, and its intensity is one magnitude higher. Secondly, the emission spectra of the germanium clusters $Ge_n{}^{p+}$ is dramatically modified. Only the atomic and dimer species (Ge^{+},$Ge_2{}^{+}$) are essentially emitted as in the pure Ge LMIS. The other pure germanium peaks have intensities that are lower and divided by a factor 100. In particular, notice that in the pure Ge LMIS the intensity ratio be-

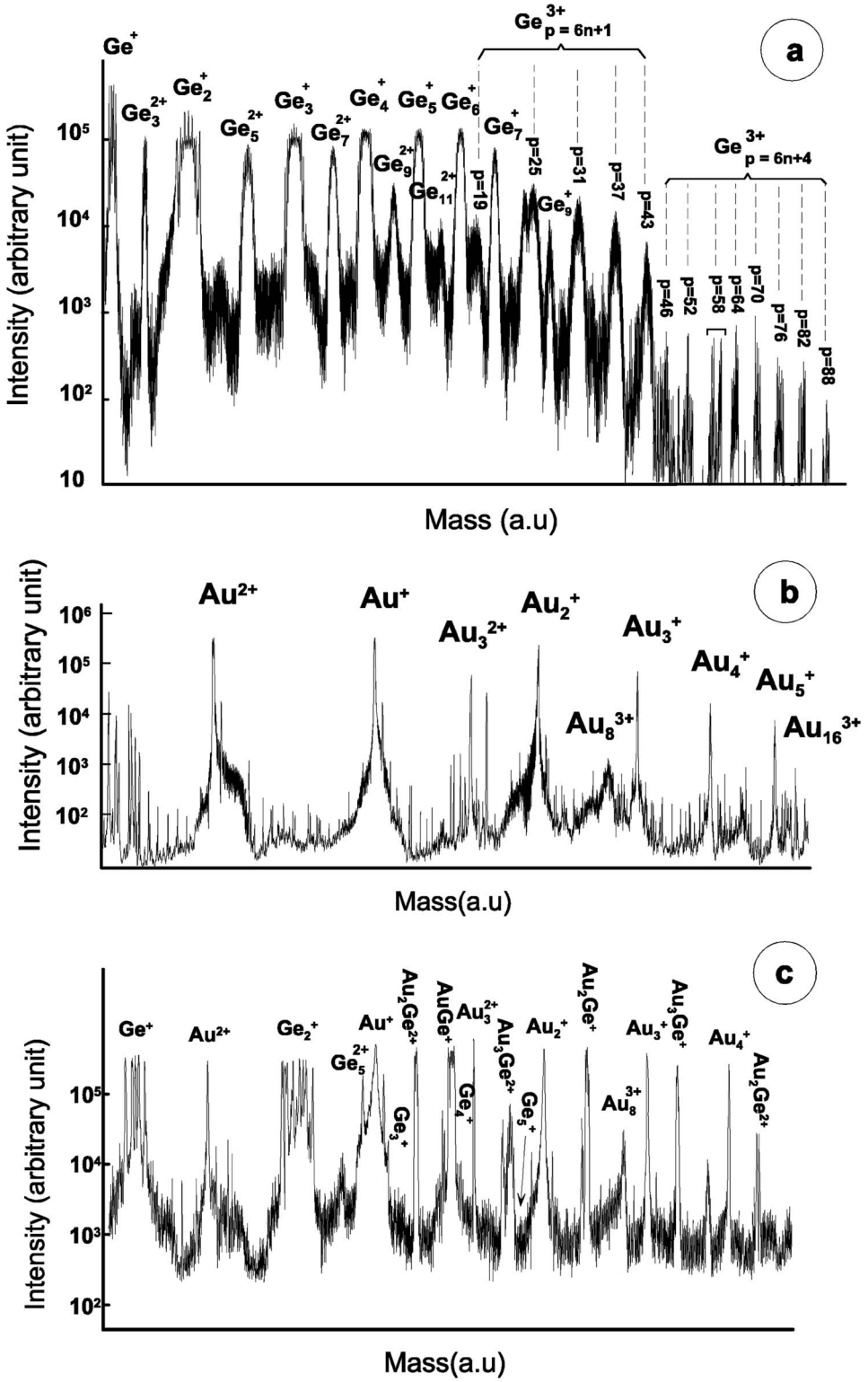

FIG. 2. LMIS mass spectrum: (a) the pure Ge case, (b) the pure Au case, and (c) the Au-Ge alloy case. Note that the different isotopic compositions in Ge clusters can clearly appear in the structure of the different peaks. The LMIS emission current is, respectively, 50, 40, and 50 μA in (a), (b), and (c).

tween the emission of Ge_3^+ and Ge_2^+ is $\simeq 1$ and in the alloy case $\simeq 0.01$. If the emission of $Ge_3^+$and Ge_2^+ were the same in the pure and alloy LMIS cases, the ratio in the alloy case would be $\simeq \frac{0.27}{0.73}$ assuming that the germanium is uniformly diluted in the alloy. Thirdly, some mixed clusters are also yielded and their compositions are $GeAu_n^{p+}$. They can be considered due to the capture of one Ge atom by a gold cluster. Let us focus our attention on the first two remarks on the emission spectra of the Au-Ge alloy LMIS. They allow to conclude to the formation of NTs with a central gold two-shell structure as in the pure Au LMIS. Due to steric arguments, it is not possible for germanium to coat the gold NT by forming a germanium shell around it. Since the relative Au/Ge dilution must be kept constant, what happens to the three germanium atoms associated to the eight gold atoms of an emitted Au_8^{3+}? As we will see below, some experimental

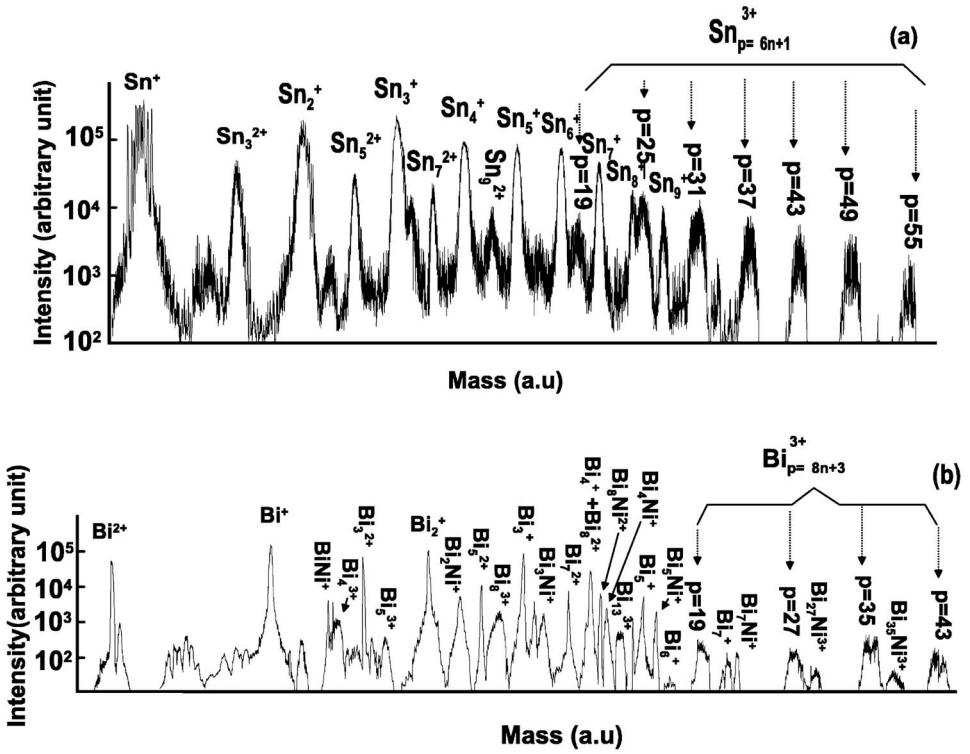

FIG. 3. LMIS mass spectrum: (a) the Sn case, (b) the Bi case. The LMIS emission current is 18 μA in (a) and (b). Ni appearing in the Bi LMIS spectra comes from the tip, which is made of an $Ni_{0.7}Fe_{0.3}$ alloy to improve the liquid wetting on it.

results suggest that they are emitted from a region B (see Fig. 1) in the vicinity of the bottom of the gold NT where the electric field is still large. Due to a relatively low concentration, they can only be emitted as Ge^+ or as Ge_2^+. The Ge_3^+ and other Ge_n^+ with $n>3$ aggregates are emitted from zones where the electric field is lower and their intensities are very weak. We must remark that though Au_8^{3+} and Ge^+, Ge_2^+ are emitted together, this does not appear in the measured intensities: the number of germanium atoms emitted in Ge^+ and Ge_2^+ is one magnitude larger than the number of gold atoms emitted in Au_8^{3+} and Au_{16}^{3+}. This fact can be the sign that either the gold emission from the tip does not involve only Au_8^{3+} but also monocharged gold species, or that it is due to the metastability of the highly charged cluster Au_8^{3+}.

The experimental data point which tends to corroborate the previous scheme is given by the isotopic composition of the peaks emitted from Au-Ge alloys. In Fig. 4, the emission of Ge_2^+ shows in the pure Ge LMIS 11 peaks and only 5 peaks in the Au-Ge alloy LMIS. The 11 peaks are associated to the set of all possible isotope diatom mixtures. The five peaks are associated to the homoisotopes of Ge_2^+. It means that a striking isotope effect is occurring for the Ge_2^+ dimers in the Au-Ge LMIS experiment. In Table I, the percentage of the dimers Ge_2^+ deduced either from the pure Ge and Au-Ge LMIS experiments or from the natural abundance is reported. Some isotopic discrepancies occur already in the pure Ge LMIS. Chiefly in the pure Ge case the experimental percentage values of the peaks 4, 6, and 8 are too small com-

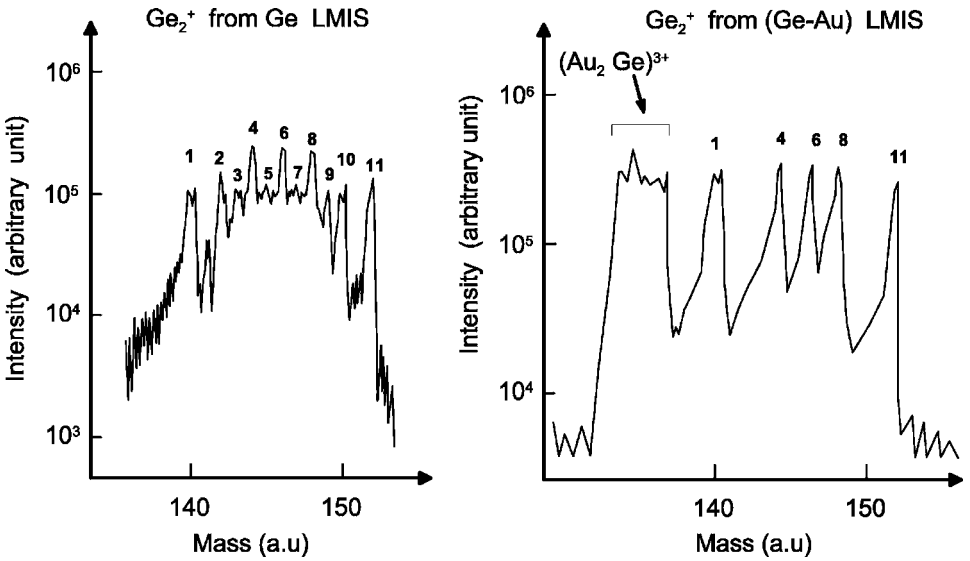

FIG. 4. Emission intensity of Ge_2^+ in either pure Ge or eutectic Au-Ge LMIS.

TABLE I. Percentage of the various Ge_2^+ isotopes in the pure Ge LMIS and the Au-Ge LMIS. The lines labeled Expt., STAT, Homo, and Hmod refer, respectively, to the experimental percentage, the natural percentage, the homoisotope natural percentage, and the natural percentage given by the homoisotopes plus 15% of dimers having a mass difference less than or equal to 2 in mass units. The lines labeled stat refer to the natural percentage of all possible dimers *ij* contributing to the peak where *i* and *j* label the Ge isotopes: ^{70}Ge(a), ^{72}Ge(b), ^{73}Ge(c), ^{74}Ge(d), ^{76}Ge(e). For instance, bd means $^{72}Ge^{74}Ge^+$.

Ge_2^+	140	142	143	144	145	146	147	148	149	150	152
Peak	1	2	3	4	5	6	7	8	9	10	11
					Ge	LMIS					
Expt.	6.83	9.63	6.8	13.6	7.65	13.6	7.6	12.1	6.83	6.83	8.54
STAT	4.21	11.25	3.18	22.52	4.26	23.85	5.67	17.60	1.20	5.67	0.60
stat	aa 4.21	ab 11.25	ac 3.18	bb 7.52	bc 4.26	cc 0.60	cd 5.67	dd 13.35	ce 1.20	de 5.67	ee 0.60
”				ad 14.99		bd 20.07		be 4.26			
”				-		ae 3.18					
					Au-Ge	LMIS					
Expt.	19.41			20.46		20.46		20.46			19.21
Homo	16.10			28.61		2.20		50.79			2.20
Hmod	12.0	4.83		21.5	1.82	17.45		38.2		2.4	1.71

pared to the natural abundance ones but for the peak 11 it is the reverse. In Table I, the various dimer contributions for each peak are reported. The peaks 4, 6, and 8 have a significant contribution of a heteroisotope dimer having a large mass difference. The relative decrease of the experimental height for the peaks 4, 6, and 8 could be interpreted already in the pure Ge case as a partial instability of these heteroisotopes. The other peaks display anomalies that are weaker and could be interpreted, except for the peak 11, also as a partial instability of heteroisotopes which is increasing with the isotope mass difference, see Table I. A process to explain the instability will be detailed later. The peak 11 will be discussed below. Let us examine the Au-Ge LMIS case. The main remark is that the Ge_2^+ peaks labeled 6 and 11 of the Au-Ge LMIS display some large discrepancies compared to the natural abundance of the homoisotopes. They are too high in comparison to the other peaks 1, 4, and 8; see Table I. Focus on the peak 6; it corresponds to mass 146. It can be produced by three different dimers: $^{73}Ge^{73}Ge^+$, $^{72}Ge^{74}Ge^+$, and $^{70}Ge^{76}Ge^+$. The intensity for the peak 6 in the Au-Ge case can be understood by adding to the homoisotope contribution one of 15–20 % of heteroisotope dimers built up with isotopes having a mass difference less than or equal to 2 mass units. The addition of this contribution does not change significantly the other peaks and improves the agreement with experiments, see Table I. Return to peak 11. Only the $^{76}Ge^{76}Ge^+$ contributes to it. In the pure Ge LMIS, the dimer peak 11 is also too high. We can put forward the following mechanism. A part of the translation energy gained during the interaction with the electric field is transformed in vibration and leads to the possibility of the dimer bond break. This effect is less important for the heaviest species because their velocities are lower. This argument could explain why the dimer peak 11 is higher than expected compared to the other dimer peaks.

As expected, the emission of the trimer Ge_3^+ displays 17 peaks in the pure Ge LMIS (Fig. 5). In the Au-Ge LMIS, the Ge_3^+ emission is weaker but we can conclude that not only the homoisotope germanium trimers but also the heteroisotope ones are formed (Fig. 5). In Table II, the percentage of the trimers Ge_3^+ deduced either from pure Ge LMIS experiments or from the natural abundance is reported. The isotopic discrepancies displayed by the trimers in the pure Ge LMIS are smaller than in the dimer case. The analysis of the various peak contributions for the trimer, in particular for the peaks 6, 8, and 10, extends the remarks made for the dimer, i.e., the trimers made of three or two different isotopes with a large mass difference seem to be also less stable.

The emission of the dimer Sn_2^+ displays 22 peaks in the pure Sn LMIS. In Table III, the percentage of the Sn_2^+ dimers deduced either from pure Sn LMIS experiments or from the natural abundance are reported. The Sn dimer isotopic discrepancies are smaller than in the Ge case, particu-

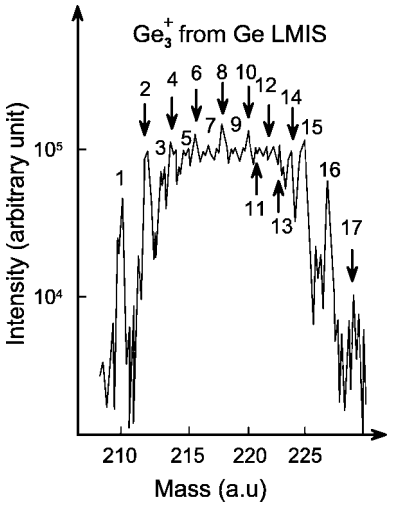

FIG. 5. Emission intensity of Ge_3^+ in pure Ge. In the inset, the eutectic Au-Ge LMIS case is shown; only the homoisotope peaks are labeled.

TABLE II. Percentage of the various Ge_3^+ isotopes in the pure Ge LMIS. The lines labeled Expt. and STAT refer, respectively, to the experimental percentage and the natural percentage.

Ge_3^+	210	212	213	214	215	216	217	218	219	220	221	222	223	224	225	226	228
Peak	1	2	3	4	5	6	7	8	9	10	11	12	13	14	15	16	17
Expt.	2.94	6.60	4.66	7.35	6.60	7.48	6.60	7.58	6.60	7.43	4.20	6.60	6.60	6.60	7.35	4.16	0.66
STAT	0.878	3.51	0.99	9.39	2.29	16.01	5.32	18.89	5.54	17.12	4.17	10.07	1.34	3.56	0.14	0.67	0.046

larly for the peak 22 corresponding to the heaviest species. The trend for Sn is in agreement with our previously mentioned arguments to explain the Ge dimer anomalies. Indeed, the Sn dimers are less excited than the Ge dimers due to an electric field at the tip smaller than in the Sn case; the respective electric field values will be discussed below.

What is the origin of this isotope effect in the Ge dimer? What is the essential difference between the pure Ge and Au-Ge LMIS? We suspect this is due to the intense electric field. In one case, a germanium NT is formed and in the other a gold NT. This difference is important for the electric field in the vicinity of the tip. In the pure Ge LMIS, the electric field is controlled by the field emission of germanium and in the Ge-Au LMIS the electric field is governed by the field emission of gold. The electric field (E) extracts the ion from the surface but it has to overcome the attractive image force. The balance between the two forces displays a maximum energy gain $(e^3E/4\pi\epsilon_o)^{1/2}$ which compensates the furnished energy $\Lambda+I-\phi$ given by the following cycle: removing one atom from the tip (the cohesive energy Λ), ionizing the atom at the infinity (the ionization potential I), and replacing the electron inside the tip (the work function ϕ). The emission field E_o is

$$E_o = \frac{4\pi\epsilon_o}{e^3}(\Lambda + I - \phi)^2. \quad (1)$$

For germanium, E_o is 3.26 V/Å, for gold 5.31 V/Å, and for Sn 2.6 V/Å. In the Au-Ge LMIS, germanium clusters are submitted to a larger electric field. One possibility to break small heteroisotope ionized clusters is associated with the inhomogeneous forces applied on each nucleus during the interaction of the ionized clusters with the intense electric field. This inhomogeneity in the force generates different acceleration on each nucleus and so different speeds provoking an increase of the bound distance (D) and finally a bond break. This effect globally increases as the cluster size decreases. This phenomenon does not happen in the Ge trimer because it is emitted from a zone with weaker electric field. LMIS provides a type of linear isotope separation. To get more quantitative insight into the origin of the isotope effect in the dimer emission in LMIS, let us investigate the behavior of a diatomic cation formed with two different isotopes in an intense local electric field as it is produced in LMIS experiments. We assume that the electric field varies along the tip axis as $E(z)=E_o\exp(-z/r_o)$ with $r_o=10$ Å. The cluster Ge_2^+ is modeled within the tight-binding approximation considering only one band. The hopping integral β and the repulsion energy E^{rep} between the nucleus are assumed to have the following typical distance dependence: $\beta\propto\exp(-D/r_{\text{hop}})$ and $E^{\text{rep}}\propto\exp(-D/r_{\text{rep}})$ with $r_{\text{hop}}=2.5$ Å and $r_{\text{rep}}=1.5$ Å. With our parameters, the bond distance is 2 Å and the dissociation energy of Ge_2^+ is $\simeq 1$ eV. The time evolution of the cluster in the intense electric field is obtained by solving numerically the Schrödinger equation. The atomic motion in the cluster is treated classically and the electronic contribution to the forces applied on the nucleus is derived with the Hellmann-Feynman theorem.[17] In Fig. 6, we report the average distance $\langle D\rangle$ in the cluster after the interaction with the electric field versus the strength of the field E_o at the tip for different Ge_2^+ with two different isotopes having a mass difference of one to six mass unit. With these parameters we can introduce a critical field that allows us to break the bond of the molecule which is defined for a bond increase of 20% and amounts to 3.2, 2.4, 1.9, 1.7, 1.5, and 1.4 V/Å to separate two isotopes when their mass difference goes, respectively, from 1 to 6 in mass units. The gold emission field being equal to 5.3 V/Å, we can guess that in re-

TABLE III. Percentage of the various Sn_2^+ isotopes in the pure Sn LMIS. The lines labeled Expt. and STAT refer, respectively, to the experimental percentage and the natural percentage.

Sn_2^+	224	226	227	228	229	230	231	232	233	234	235
Peak	1	2	3	4	5	6	7	8	9	10	11
Expt.	0.186	0.0744	0.166	0.66	0.47	1.32	1.05	4.71	4.189	7.44	6.65
STAT	0.094	0.0126	0.0066	0.286	0.15	0.66	0.365	3.108	2.507	8.20	6.43
Sn_2^+	236	237	238	239	240	241	242	243	244	246	248
Peak	12	13	14	15	16	17	18	19	20	21	22
Expt.	13.23	8.36	13.23	6.65	10.50	3.73	5.925	2.966	4.7	1.86	1.86
STAT	16.83	9.19	17.94	6.348	14.54	1.68	5.822	0.994	3.98	0.536	0.335

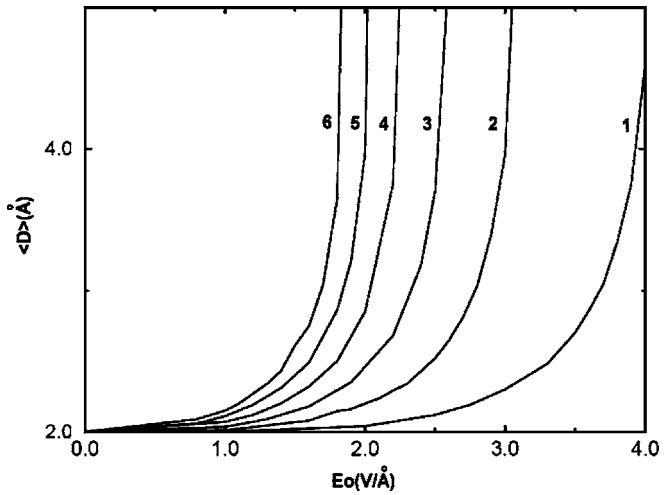

FIG. 6. Average bond distance $\langle D \rangle$ in a heteroisotope diatomic Ge_2^+ cluster after the interaction with an electric field $[E(z) = E_o \exp(-z/r_o)$ with $r_o = 10$ Å$]$ vs E_o. The curves are labeled by the mass difference between the two isotopes in mass unit.

gion B (Fig. 1) the value of the electric field required to break the bond of Ge_2^+ is achieved.

In conclusion, LMIS experiments show that an intense electric field can stretch NTs built up with elements such Ge, Sn, and Au. To confirm our interpretation, we suggest two types of experiments. First the visualization of NTs at the LMIS apex, which is not easy but is feasible due to the recent improvements in HRTEM (beam stability, etc.). Secondly, by the studies of the clusters emitted from the NT (Ge_{6n+1}^{3+}, Ge_{6n+4}^{3+}) to get more insights, chiefly on their geometric structures. The clusters could either be trapped to measure their vibration frequencies by IR spectroscopy or be deposited by soft landing to form a film. In the former case, the properties both of the individual cluster and of the film are of great interest. For experimental reasons, only the eutectic-alloy LMIS has been examined. The dependence of the tip structure on the Au-Ge alloy concentration could be an interesting study. It seems obvious that at low gold concentration, germanium NTs are formed, and conversely at high gold concentration gold NTs. How is the transition between these two regimes as the alloy concentration varies? In our Cu LMIS, the cluster Cu_8^{3+} is not found. This means that in our interpretation, Cu NTs are not formed. The result is in agreement with the Leiden experiments[8] on the absence of NWs for 3*d* and 4*d* metals. However, it would be important to confirm this point for other 3*d* elements in LMIS. NT formation in LMIS leads to new interesting features like the mentioned isotope emission anomaly for a Ge dimer, which could be viewed as a special chemical reaction where the reaction channel is controlled by NTs. We hope to find other chemical processes that can also be influenced by NTs.

The authors thank Pascal Lederer for his help.

[1] S. Iijima, Nature (London) **354**, 56 (1991).
[2] Y. Kondo and K. Takayanagi, Sciences (N.Y.) **289**, 606 (2000).
[3] V. Rodrigues, T. Fuhrer, and D. Ugarte, Phys. Rev. Lett. **85**, 4124 (2000).
[4] Y. Oshima, H. Koizumi, K. Mouri, H. Hirayama, K. Takayanagi, and Y. Kondo, Phys. Rev. B **65**, 121401 (2002).
[5] C. J. Muller, J. M. van Ruitenbeek, and L. J. de Jongh, Phys. Rev. Lett. **69**, 140 (1992).
[6] A. I. Yanson, I. K. Yanson, and J. M. van Ruitenbeek, Nature (London) **400**, 144 (1999).
[7] D. F. Urban, J. Bürki, C.-H. Zhang, C. A. Stafford, and H. Grabert, Phys. Rev. Lett. **93**, 186403 (2004).
[8] R. H. M. Smit, C. Untiedt, A. I. Yanson, and J. M. van Ruitenbeek, Phys. Rev. Lett. **87**, 266102 (2001).
[9] E. Tosatti, S. Prestipino, S. Kostlmeier, A. Dal Corso, and F. D. Di Tolla, Science **291**, 288 (2001).
[10] J. Van de Walle, R-J. Tarento, and P. Joyes, Phys. Rev. B **54**, 261 (1996).
[11] G. Benassayag, P. Sudraud, and B. Jouffrey, Ultramicroscopy **16**, 1 (1985).
[12] D. R. Kingham and L. W. Swanson, Appl. Phys. A **34**, 123 (1984).
[13] G. Forbes, Vacuum **48**, 85 (1997).
[14] P. Joyes and J. Van de Walle, J. Phys. (Paris) **47**, 821 (1986).
[15] J. Van de Walle and P. Joyes, J. Phys. (Paris) **46**, 1223 (1985).
[16] J. Van de Walle and P. Joyes, Phys. Rev. B **35**, 5509 (1987).
[17] R. P. Feyman, Phys. Rev. **56**, 340 (1939).